

Examining the Modes of Activity of
Novel Pro-death Molecules

A thesis submitted by

Shiyun Wang

in partial fulfillment of the requirements for the degree of

Master of Science

in

Pharmacology and Drug Development

Tufts University

Graduate School of Biomedical Sciences

May 2021

Advisor: Alexei Degterev, Ph.D.

Abstract

Programmed cell death regulates physiological processes and maintains cellular homeostasis. It is crucial to regulate and avoid insufficient or unrestrained cell death in cancer, inflammation, and neurodegeneration. RIPK1 and IAPs are key mediators in the cell death pathway. SMAC mimetics are IAP antagonists that induce caspase activation and promote cell death. Here, we investigated the synergistic effect of SMAC mimetic birinapant and RIPK1 inhibitor CS3 on the cell death pathway. Results are presented that CS3 and birinapant triggered a combination of cell death consisting of apoptosis and pyroptosis, which was dependent on RIPK1. CS3 and birinapant caused degradation of RIPK1 and XIAP. Other RIPK1 inhibitors, GSK'547 and GSK'481, interfered with cell death induced by CS3 and birinapant. We also focused on the cellular mechanism of a novel series of RIPK3 inhibitor analogs that potently activate necroptosis. By constituting human MLKL, murine MLKL, and its mutants into MLKL^{-/-} MEFs, we determined the different cell survival responses by different analogs. Among all of the analogs, UH15-22 was selected due to its high sensitivity and low toxicity. The MLKL mutations of M272W and S462A were found to partially block the necroptotic cell death, indicating that these residues were involved in the interaction between RIPK3 and MLKL. In addition, UH15-22 induced the release of exosomes, which required both RIPK3 and MLKL.

Table of Contents

Title Page	i
Abstract	ii
Table of Contents	iii
List of Figures	v
List of Abbreviations	vi
Chapter 1: Introduction	1
1.1. Overview of apoptotic and necroptotic cell death pathways	1
1.2. Effects of CS3/birinapant-mediated cell death	2
1.2.1. Anti-cancer pro-apoptotic activity of SMAC mimetic - Birinapant	2
1.2.2. Type 2 RIPK1 inhibitors - Ponatinib and CS series	4
1.3. Roles of RIPK3 and MLKL in necroptosis	4
1.4. Earlier work - Birinapant/CS3 and inducers of necroptosis	5
Chapter 2: Methods and Materials	7
2.1. Cell lines and cell culture	7
2.2. Generation of stable cell lines using CRISPR/Cas9 system	7
2.3. Viability assay	7
2.4. Western blotting	8
2.5. Extracellular vesicle extraction	8
2.6. Real-time qPCR	9
2.7. Statistical analysis	9
Chapter 3: Results	10
3.1. CS3/birinapant-mediated cell death	10
3.1.1. CS3 and birinapant induced pyroptosis and apoptosis	10
3.1.2. RIPK1 and IAPs are key regulators in CS3/birinapant-mediated cell death	10
3.1.3. Individual HeLa cells have different sensitivity to CS3 and birinapant	13
3.2. Activation of necroptosis by UH15 and ALD analogs	14
3.2.1. RIPK3 inhibitors had different toxicities	14
3.2.2. Key residues involved in RIPK3 and MLKL interaction	15
3.2.3. Release of exosomes in response to UH15-22 mediated by RIPK3 and MLKL	17

Chapter 4: Discussion	19
4.1. Possible mechanisms of CS3/birinapant-mediated cell death	19
4.2. Putative effects of UH15 and ALD analogs on RIPK3 and MLKL	19
4.3. Future directions	20
Chapter 5: Bibliography	21

List of Figures

Figure 1.1. TNF α -mediated cell survival and cell death pathways	2
Figure 1.2. SMAC mimetic binds to IAPs and inhibits their activities in induction of Apoptosis	3
Figure 1.3. Mechanism of RIPK3/MLKL-mediated necroptosis	5
Figure 3.1. The cell death induced by CS3 and birinapant in HeLa cells requires RIPK1	11
Figure 3.2. XIAP deficiency triggered TNF α release in birinapant-mediated cell death	12
Figure 3.3. Heterogeneity of cell sensitivity toward CS3 and birinapant in HeLa cells ..	13
Figure 3.4. RIPK3 inhibitor analogs present different toxicities.....	15
Figure 3.5. Residues Met ²⁷² and Ser ⁴⁶² in murine MLKL affect necroptosis activation....	16
Figure 3.6. Release of exosomes induced by UH15-22 requires the presence of RIPK3 and MLKL.....	18

List of Abbreviations

BIR - Baculovirus inhibitor of apoptosis protein repeat
CARD - Caspase recruitment domain
cIAP- Cellular inhibitor of Apoptosis protein
CYLD - Cylindromatosis
DAMPs - Damage-associated molecular patterns
ESCRT - Endosomal sorting complexes required for transport
EVs - Extracellular vesicles
FADD - FAS-associated death domain protein
HB - Helix bundle
ITCH - Itchy E3 ubiquitin protein ligase
LUBAC - Linear ubiquitin chain assembly complex
MEFs - Mouse embryonic fibroblasts
MLKL - Mixed lineage kinase domain-like pseudokinase
NF- κ B - Nuclear factor kappa-light-chain-enhancer of activated B cells)
PAMPs - Pathogen-associated molecular patterns
PROTAC - Proteolysis targeting chimera
RAB5 - Ras-related protein Rab-5
RING - Really interesting new gene
RIPK - Receptor-interacting serine-threonine-protein kinase
RHIM - Receptor-interacting protein homotypic interaction motif
SMAC - Second mitochondria-derived activator of caspase
TNF - Tumor necrosis factor
TNFR1 - Tumor necrosis factor receptor 1
TSG101 - Tumor susceptibility gene 101
UBA - Ubiquitin-associated
VAMP7 - Vesicle-associated membrane protein 7
XIAP - X-linked inhibitor of apoptosis

Chapter 1: Introduction

1.1. Overview of apoptotic and necroptotic cell death pathways

Programmed cell death is an essential physiological process to maintain normal development and cellular homeostasis. In various pathological processes such as cancer, inflammatory diseases, and neurodegenerative disorders, it contributes to inadequate or excessive cell death under different circumstances.¹ Currently, multiple types of programmed cell death pathways have been discovered and characterized, two of which are apoptosis and necroptosis. Apoptosis is characterized by specific morphological changes whereby cytoplasm and chromatin are condensed in dying cells and then phagocytosed by neighboring cells.² Distinguished from apoptotic cells, necroptotic cells undergo plasma membrane disruption, organelle breakdown, and intracellular content leakage.³⁻⁴

While the cell death pathway can be triggered by various stimuli, the best characterized one is the TNF α -mediated cell death pathway (Fig 1.1). Upon TNF α binding to TNFR1, multiple proteins are recruited to TNFR1 to form membrane-associated complex I, within which the polyubiquitination of RIPK1 is promoted by cIAP1/2 and LUBAC. The ubiquitinated RIPK1 activates the NF- κ B pathway, resulting in inflammatory responses and cell survival. Deubiquitination of RIPK1 by A20 or CYLD causes dissociation of it from TNFR1 and induces the binding to FADD to form complex II. Caspase 8 is recruited to complex II to activate the apoptotic response. In the case when caspase 8 is inhibited, RIPK1 dissociates from complex II and phosphorylates RIPK3, which can then induce the phosphorylation and

oligomerization of MLKL. MLKL then translocates to the plasma membrane, compromising the plasma membrane integrity and inducing necroptotic responses.⁴⁻⁶

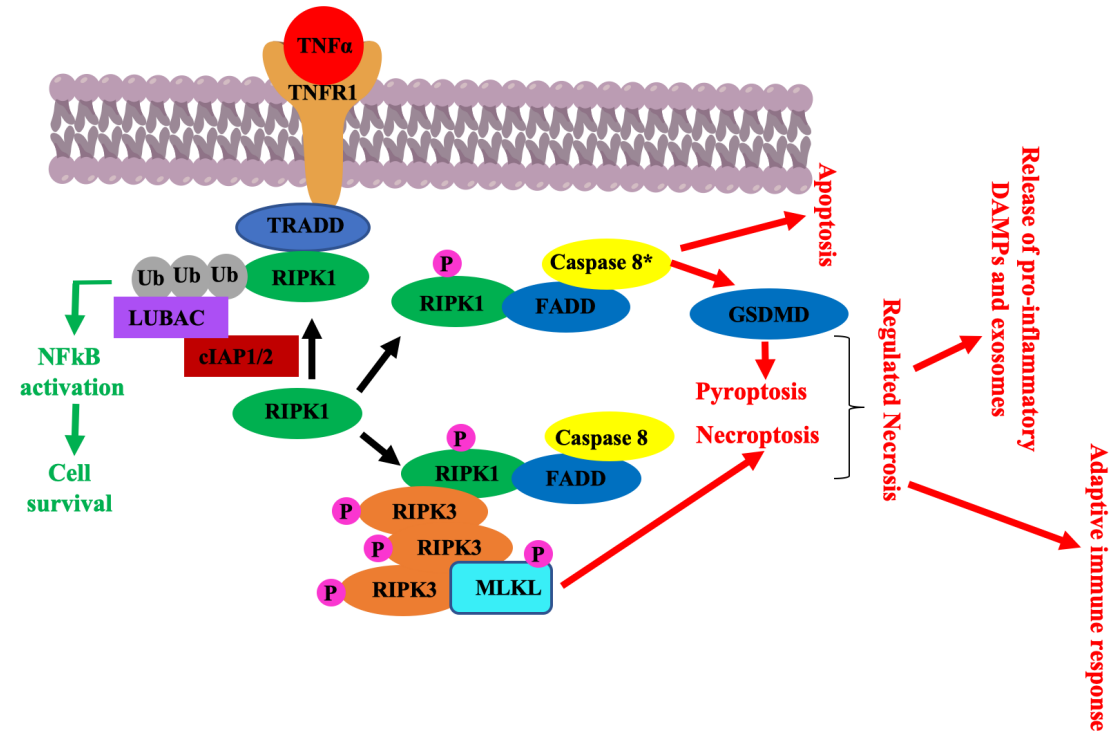


Figure 1.1. TNF α -mediated cell survival and cell death pathways.

1.2. Effects of CS3/birinapant -mediated cell death

1.2.1. Anti-cancer pro-apoptotic activity of SMAC mimetic - Birinapant

IAPs are among the crucial regulators in the cell death pathway. These proteins contain three BIR domains, one UBA domain, and one RING domain. cIAP1/2 also contain a CARD domain.⁷⁻⁸ Specifically, XIAP directly binds to caspases and inhibits their activities while cIAP1/2 are more involved in the ubiquitination of RIPK1 and interference of complex II formation.⁷ SMAC, a protein localized at the inner mitochondrial membrane and released into cytosol upon pro-death stimuli, binds to BIR3

domain of XIAP and promotes apoptosis.^{1,8-9} SMAC mimetics are designed based on the N-terminal Ala1-Val2-Pro3-Ile4 (AVPI) tetrapeptide binding motif and imitate the inhibitory function of endogenous SMAC on IAPs, triggering apoptosis in cancer treatment.⁹⁻¹¹ Most SMAC mimetics, initially designated to inhibit XIAP, turned out to have higher binding affinity to cIAPs.^{9,11} Furthermore, these molecules were found to cause cIAP1/2 auto-ubiquitination and degradation, unleashing a pro-death cascade involving TNF α synthesis through a non-canonical NF- κ B signaling pathway and TNF α -dependent apoptosis (Fig. 1.2). Birinapant, as one of the novel SMAC mimetic compounds that binds more specifically to and antagonizes cIAP1, thus potentially improving safety. Currently, due to its potential therapeutic effect, birinapant is under investigation as a single agent or in combination therapy with chemotherapeutic drugs and radiotherapy for treatment of cancers including acute myeloid leukemia, melanoma, glioblastoma, and breast cancer.¹²

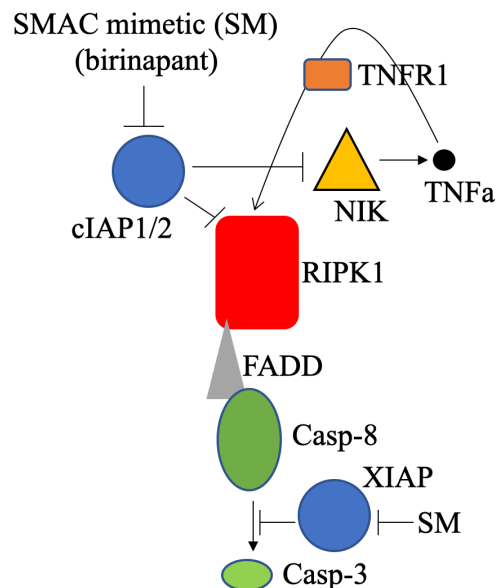


Figure 1.2. SMAC mimetic binds to IAPs and inhibits their activities in induction of apoptosis.

1.2.2. Type 2 RIPK1 inhibitors - Ponatinib and CS series

Ponatinib is a BCR-ABL tyrosine kinase inhibitor intended to treat patients with chronic myeloid leukemia and Philadelphia chromosome-positive acute lymphoblastic leukemia.¹³⁻¹⁴ Previous research has identified ponatinib as a dual inhibitor of RIPK1 and RIPK3 that blocks necroptotic activity.¹³ Based on the structure of ponatinib, CS series compounds were generated by introducing bulkier substitutes at central phenyl ring to enhance their selectivity toward RIPK1 and RIPK3.¹⁵ The inhibitory effect of CS series against RIPK1 was confirmed by our previous results.¹⁵ CS3, with an addition of n-propyl substituent on RING A, induced apoptotic cell death synergistically upon treatment with birinapant as I will discuss below.

1.3. Roles of RIPK3 and MLKL in necroptosis

Components of necrosome, which consist of RIPK1, RIPK3, and MLKL, are critical mediators in the necroptotic cell death pathway. The deubiquitination of RIPK1 induces the interaction between RIPK1 and RIPK3 through their RHIM domains and formation of β -amyloid structures.¹⁶⁻¹⁷ As shown in Fig 1.3, after activation by autophosphorylation within the RIPK1/RIPK3 heterodimeric functional amyloid signaling complex, RIPK3 induces the phosphorylation and oligomerization of MLKL.¹⁶ MLKL phosphorylation promotes its conformational change by releasing 4HB domain and stabilizing the interaction between kinase domain of RIPK3 and pseudokinase domain of MLKL.^{16,18} MLKL then aggregates from monomers to higher-order entities that are translocated to the plasma membrane to mediate plasma membrane permeabilization.¹⁷ The interaction between RIPK3 and MLKL, as a result, is significant for the initiation and regulation in necroptotic cell death pathway.

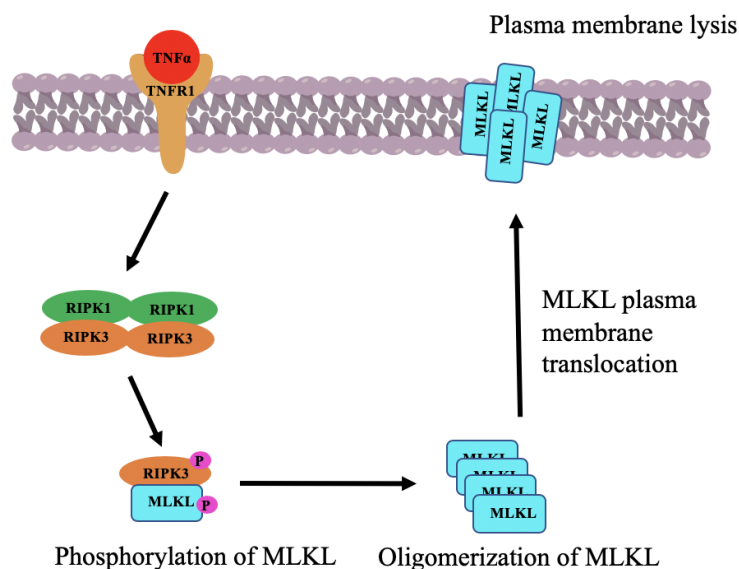


Figure 1.3. Mechanism of RIPK3/MLKL-mediated necroptosis.

1.4. Earlier work - Birinapant/CS3 and inducers of necroptosis

Previously, our lab tested the co-treatment of birinapant with six different CS series drugs (CS1-6) and the results indicated that the treatment of birinapant with any one of the CS series drugs induced cell death. Following on from the previous work, this thesis will continue focusing on the regulation of proteins that occur in CS3/birinapant-mediated cell death and the heterogeneity of sensitivity in different clones induced by CS3 and birinapant.

Previous efforts confirmed the essential roles of RIPK3 and MLKL in necroptotic cell death induced by new small molecule activators of RIPK3/MLKL developed in the lab - UH15-22 and ALD-4-75. Based on the preceding outcome, this thesis will further investigate on functions of RIPK3 and MLKL in necroptotic cell death pathway, specifically including the differential sensitivities to necroptosis induced by multiple analogs of RIPK3 inhibitor, key residues in MLKL that contribute to the interaction

between RIPK3 and MLKL, and exosomes release upon the activation of RIPK3 and MLKL.

Figure 1.1 and 1.2 were made by Dr. Alexei Degterev. Figure 1.3 was made by myself.

Chapter 2: Methods and Materials

2.1. Cell lines and cell culture

HeLa cells were cultured in Dulbecco's Modified Eagle's Medium (Corning) supplemented with 10% fetal bovine serum (Sigma-Aldrich), 1% penicillin-streptomycin (Gibco), and 100 µg/mL Normocin (InvivoGen). MEFs were cultured in DMEM supplemented with 10% FBS, 1% penicillin-streptomycin, 10 µM HEPES (cytiva), 1mM Sodium Pyruvate (gibco), and 1% MEM Non-Essential Amino Acids Solution (gibco). RAW 264.7 cells were cultured in DMEM supplemented with 10% fetalplex (Gemini), 1% penicillin-streptomycin, and 25 µg/mL Plasmocin (InvivoGen). HEK293T cells were cultured in DMEM supplemented with 10% FBS, 1% penicillin-streptomycin, and 25 µg/mL Plasmocin. All cells were maintained at 37°C incubator with 5% CO₂.

2.2. Generation of stable cell lines using CRISPR/Cas9 system

All LentiCRISPR v2 plasmids cloned by corresponding gRNAs were cotransfected with pMD2.G (Addgene plasmid #12259) and psPAX2 (Addgene plasmid #12260) into HEK293T using transfection reagent Lipofectamine 2000 (Invitrogen). HeLa cells, MEFs, and RAW 264.7 cells were transduced with lentiviruses containing above-mentioned gRNA sequences and selected 48 hr after transduction with either puromycin, blasticidin or hygromycin B Gold.

2.3. Viability assay

3.5×10^3 HeLa cells were seeded into a 96-well plate per well and treated with either DMSO or indicated concentrations of CS3 and Birinapant on the following day. 3.5×10^3 MEFs were seeded into a 96-well plate per well and treated with doxycycline on the next morning and either DMSO or indicated concentrations of UH15 analogs or ALD

analogs after 6 hr of doxycycline treatment. Cell viability was assessed after 24 hr treatment by CellTiter-Glo Luminescent Cell Viability Assay (Promega) following the manufacturer's instructions.

2.4. Western blotting

Cells were collected and lysed in radioimmunoprecipitation assay (RIPA) buffer with 50 µg/mL phenylmethylsulfonyl fluoride (PMSF). Cell lysates were sonicated twice and centrifuged at 14,000 rpm for 15 min at 4°C. Protein concentration was measured by Pierce 660nm Protein Assay Reagent (ThermoFisher) and normalized. Proteins were boiled in 4X SDS sample loading buffer, separated by SDS-PAGE gel, transferred to PVDF membranes (Bio-Rad), and probed with the following antibodies overnight at 4°C: alpha tubulin (Proteintech, Cat No. 11224-1-AP; 1:5000), RIPK1 (Cell Signaling, Cat No. 3493; 1:1000), XIAP (Cell Signaling, Cat No. 2045; 1:1000), GSDME (abcam, Cat No. ab215191; 1:1000), Caspase 3 (Cell Signaling, Cat No. 9662; 1:1000), Caspase 8 (Cell Signaling, Cat No. 9746; 1:1000), RIPK3 (Prosci; 1:1000), MLKL (Millipore, Cat No. MABC604; 1:1000), CD63 (Novus, Cat No. NBP2-32830; 1:500), ITCH (BD, Cat No. 611198; 1:1000), VAMP7 (Cell Signaling, Cat No. 14811; 1:1000), TSG101 (Novus, Cat No. NBP2-77452; 1:1000), RAB5 (abcam, Cat No. ab218624; 1:1000). HRP-linked secondary antibodies (Cell Signaling; 1:5000) were incubated for 1 hr at room temperature followed by immunoblotting using Immobilon western HRP substrate (Millipore).

2.5. Extracellular vesicle extraction

EVs extraction was performed using Gerlic protocol.¹⁹ 7×10^6 RAW 264.7 cells were seeded in serum-free DMEM and treated with 2.5 µM UH15-22 overnight.

Supernatant was collected, centrifuged at 400 x g for 5 min to pellet cells, and further centrifuged at 1,500 x g for 5 min to remove debris. Supernatant was then centrifuged at 14,000 x g for 70 min at 4°C to remove microvesicles and filtered through a 0.45 µm filter. The flow through was collected and centrifuged at 100,000 x g for 190 min at 4°C to pellet EVs. Supernatant was again centrifuged at 100,000 x g overnight at 4°C to pellet smallest EVs. Pelleted EVs were resuspended in 100 µL PBS, diluted in 33 µL 4X SDS sample loading buffer, boiled for 5 min, and loaded onto SDS-PAGE gel for further analysis.

2.6. Real-time qPCR

Total RNA was isolated from cells using Quick RNA Miniprep Kit (Zymo) and complementary DNA was amplified by reverse transcription PCR using iScript cDNA synthesis kit (Bio-Rad) according to the manufacturer's protocol. Real-time qPCR was performed to obtain the nucleotide products using SsoAdvanced Universal SYBR Green Supermix (Bio-Rad).

2.7. Statistical analysis

All data were presented as mean with SD. Two-way ANOVA was performed by Prism 8.4.3 to compare the statistical differences between different groups. Statistical significance is presented as *n.s.*, not significant; *, $p < 0.05$; **, $p < 0.01$; ***, $p < 0.001$; ***, $p < 0.0001$.

Chapter 3: Results

3.1. CS3/birinapant-mediated cell death

3.1.1. CS3 and birinapant induced pyroptosis and apoptosis

Our previous results indicated that the combination of CS3 and birinapant induced cell death in HeLa cells. To investigate the specific type of cell death triggered by CS3 and birinapant, markers of different types of cell death pathway were tested. CS3 and birinapant-treated HeLa cells showed cleavage of caspase 3 and caspase 8, indicating the activation of apoptotic cell death pathway. The N-terminal fragment of GSDME was elevated as induced by CS3 and birinapant, which suggested that pyroptosis was also involved in the CS3/birinapant-mediated cell death (Fig. 3.1A).

In previous experiments, two of the key regulators in the cell death pathway, RIPK1 and XIAP were found to be degraded in HeLa cells induced with CS3 and birinapant (Fig. 3.1A). To test whether the degradation was associated with proteasome, proteasome inhibitor bortezomib was used in HeLa cells in addition to CS3 and birinapant. The result showed that bortezomib blocked the degradation of RIPK1 and XIAP induced by CS3 and birinapant (Fig. 3.1B), confirming that the degradation of RIPK1 and XIAP was proteasome-dependent.

3.1.2. RIPK1 and IAPs are key regulators in CS3/birinapant-mediated cell death

Since RIPK1 and XIAP were degraded under the treatment of CS3 and birinapant, it was hypothesized that RIPK1 and XIAP were essential for CS3/birinapant-mediated cell death. RIPK1-knockout HeLa cells were generated using the lentiviral CRISPR/Cas9 system. RIPK1 deficiency in HeLa cells inhibited the cleavage of caspase 3, caspase 8, and GSDME and partially prevented the degradation of XIAP under the treatment of CS3

and birinapant (Fig. 3.1A). RIPK1 deficiency protected HeLa cells from being killed by birinapant alone or CS3 and birinapant (Fig. 3.1C). Collectively, these results indicated that RIPK1 is required in CS3/birinapant-mediated cell death. Given the previous result that CS3 acts as an antagonist of RIPK1, to consolidate the assumption that CS3 binds to RIPK1 to induce cell death, other RIPK1 inhibitors, GSK'547 and GSK'481, were used to treat HeLa cells in addition to CS3 and birinapant. The results showed that both GSK'547 and GSK'481 protected the HeLa cells when treated with birinapant alone or with birinapant and CS3 (Fig. 3.1D), which suggested that GSK'547 and GSK'481 may bind to and protect RIPK1 from being regulated in CS3/birinapant-mediated cell death.

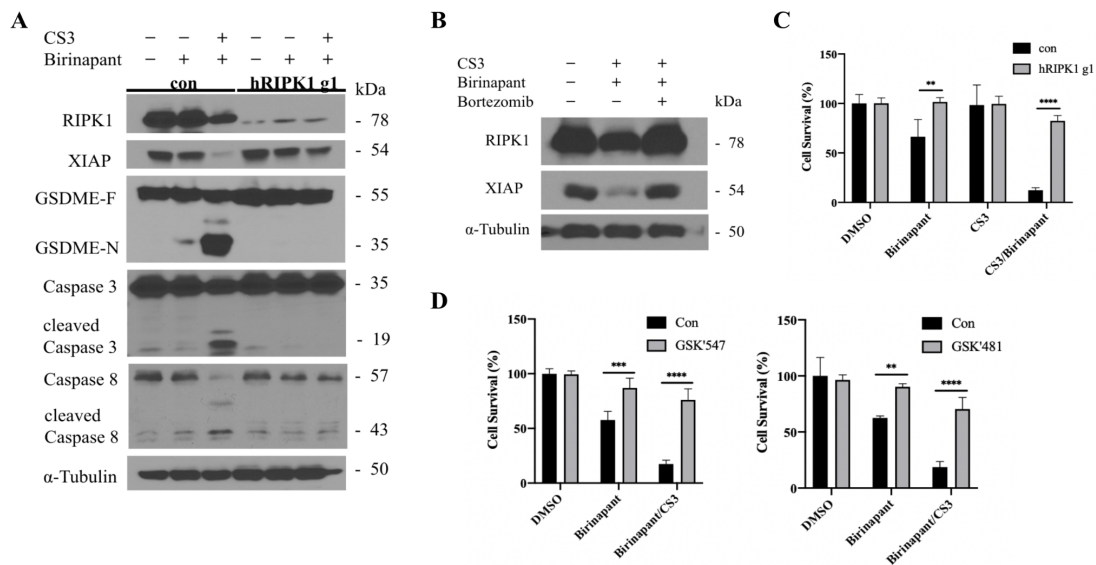


Fig 3.1. The cell death induced by CS3 and birinapant in HeLa cells requires RIPK1. (A) HeLa control and hRIPK1-knockout cells were treated with or without 10 nM birinapant and 1 μ M CS3 for 24 hr. GSDME, caspase 3, caspase 8, their cleaved forms, RIPK1 and XIAP expression levels were determined by western blot analysis. (B) HeLa wild-type cells were treated with or without 100 nM birinapant, 1 μ M CS3, and 1 μ M bortezomib for 24 hr. RIPK1 and XIAP were analyzed by western blot. (C) HeLa control and hRIPK1-knockout cells were treated with or without 1 μ M birinapant and 1 μ M CS3 for 24 hr. (D) HeLa wild-type cells were treated with or without 50 nM birinapant, 10 nM birinapant and 1 μ M CS3, and 250 nM GSK'547 or GSK'481 for 24 hr. Cell survival was measured by ATP assay. All the data are presented as mean \pm SD of n = 3 using two-way ANOVA with Sidak's multiple comparison test.

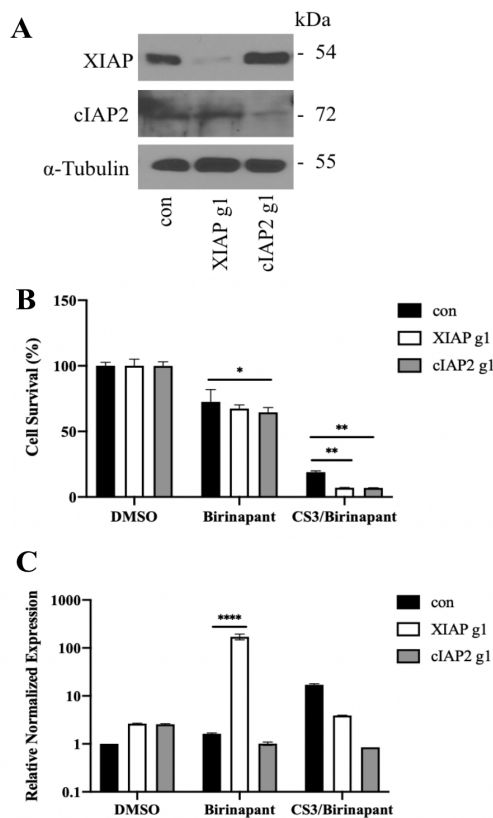


Fig. 3.2. XIAP deficiency triggered TNF α expression in birinapant-mediated cell death. (A) HeLa cells were transduced with XIAP g1 construct or cIAP2 g1 construct to generate XIAP-knockout and cIAP2-knockout cells. Expression level was analyzed by western blot. (B) HeLa control (con), XIAP-knockout, and cIAP2-knockout cells were treated with or without 100 nM birinapant and 1 μ M CS3 for 24 hr. Cell survival was measured by ATP assay. (C) The mRNA level of TNF α in HeLa con, XIAP-knockout, and cIAP2-knockout cells treated with or without 10 nM birinapant and 1 μ M CS3 for 16 hr was measured by qRT-PCR. All the data are presented as mean \pm SD of n=3 using Two-way ANOVA with Dunnett's multiple comparison test.

IAPs may serve as E3 ligases that account for degradation of XIAP and RIPK1. Therefore, XIAP-knockout and cIAP2-knockout HeLa cells were also generated to investigate the function of IAPs in CS3/birinapant-mediated cell death pathway. The expression levels of XIAP and cIAP2 were confirmed (Fig. 3.2A). Cell survival rates were reduced in HeLa cells with XIAP or cIAP2 deficiency compared to the control group (Fig. 3.2B), indicating that XIAP and cIAP2 may have protective functions that prevent cell death induced by CS3 and birinapant.

Due to the fact that multiple cell signaling pathways including NF- κ B cell survival pathway and apoptosis are triggered by TNF α binding to TNFR1, the level of TNF α was measured to see whether it may account for the CS3/birinapant-mediated cell

death. IAPs, as key mediators in the TNF α -mediated cell death pathway, were inhibited to investigate their impact on TNF α release. The results suggested that only XIAP-deficient HeLa cells treated with birinapant exhibited a significantly elevated level of TNF α (Fig 3.2F).

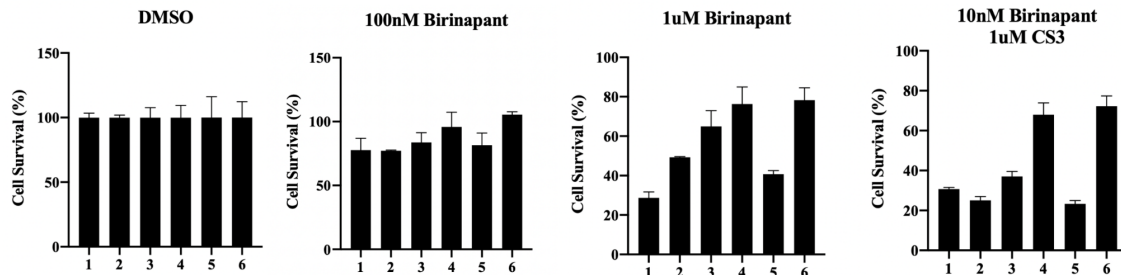


Fig. 3.3. Heterogeneity of cell sensitivity toward CS3 and birinapant in HeLa cells. HeLa clone 1-6 were treated with DMSO or indicated concentrations of birinapant and CS3 for 24 hr and the survival rate was determined by ATP assay. All the data are presented as mean \pm SD of n = 2.

3.1.3. Individual HeLa cells have different sensitivity to CS3 and birinapant

When selecting single cell clones from transduced cells for a complete CRISPR knockout clone of genes mentioned before, we noticed that different clones with comparable protein expression levels had discrepant responses to CS3 and birinapant, leading to the assumption that the different sensitivity observed in each clone might result from the heterogeneous nature of HeLa cells instead of the protein expression level alone. In order to substantiate the aforementioned assumption, six single clones of HeLa cells were picked and expanded. Indeed, the result showed that single clones responded to birinapant alone or to co-treatment of CS3 and birinapant differently, especially at 10 nM birinapant and 1 μ M CS3 (Fig. 3.3). Therefore, it is important to take the heterogeneity of

HeLa cells into account and eliminate it by selecting a single clone from the total population of HeLa cells.

3.2. Activation of necroptosis by UH15 and ALD analogs

3.2.1. RIPK3 inhibitors had different toxicities

While previous publications indicated that necroptosis is activated through the interaction between the kinase domain of RIPK3 and the pseudokinase domain of MLKL, the specific activation mechanism induced by conformational change is still not well understood.^{16,18} A novel series of necroptosis inducers, UH15/ALD analogs, were identified to bind RIPK3 and MLKL and to induce caspase-independent cell death. However, the mechanism of action of these molecules remains incompletely understood. In my experiments, the roles of MLKL were first focused. Because human MLKL does not interact with murine RIPK3, MLKL^{-/-} MEFs re-expressing human MLKL were generated under the control of a doxycycline-inducible promoter. 5 uM necroptosis inducers activated necroptotic cell death in MEFs re-expressing human MLKL, which could be protected by MLKL deficiency (Fig 3.4), confirming the essential and sufficient role of MLKL in necroptosis. UH15 analogs all promoted cell death in the presence of MLKL, but with different efficiencies: UH15-30, ALD-6-4, and ALD-6-1 started to induce cell death at 0.625 uM (Fig 3.4B, C, and F) whereas ALD-4-60 only triggered cell death at 5 uM (Fig. 3.4D). Together, the results presented above showed different potency toward different analogs of RIPK3, which may result from different binding affinity caused by structural differences in each analog of RIPK3 inhibitor.

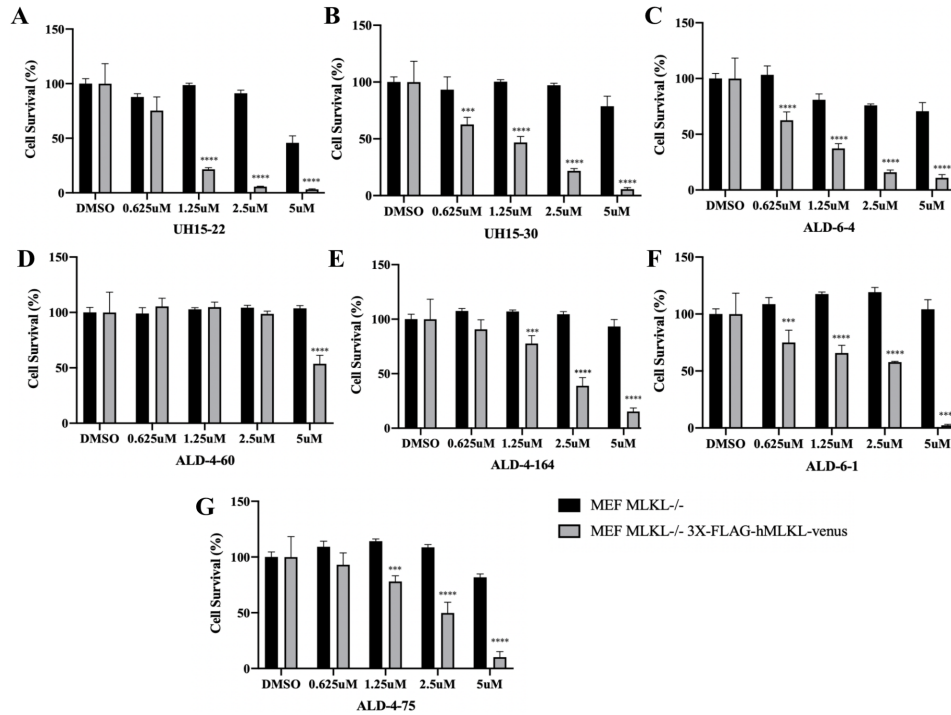


Fig. 3.4. RIPK3 inhibitor analogs present different toxicities. MEFs were treated with 5 ng/mL doxycycline 6 hr prior to the indicated concentrations of RIPK3 inhibitors, (A) UH15-22, (B) UH15-30, (C) ALD-6-4, (D) ALD-4-60, (E) ALD-4-164, (F) ALD-6-1, (G) ALD-4-75. Survival rate was measured 24 hr after treatment by ATP assay. All the data are presented as mean \pm SD of $n = 3$ using Two-way ANOVA with (A) Bonferroni's multiple comparison test or (B-G) Sidak's multiple comparison test.

3.2.2. Key residues involved in RIPK3 and MLKL interaction

The binding interaction between RIPK3 and MLKL is mainly mediated by the pseudokinase domain of MLKL, but the selective engagement of RIPK3 to MLKL is also at least partially dictated by other residues within MLKL.¹⁸ Based on our docking results, Met²⁷² and Ser⁴⁶² are two of the key residues which may contribute to the binding interaction between RIPK3 and MLKL that triggers necroptosis based on the molecular modeling performed by our collaborators in Dr. Gregory Cuny's lab (University of Houston). Met²⁷², located at the N-lobe of pseudokinase domain, controls access into the MLKL pseudo-active center.²⁰ Ser⁴⁶², located in the brace region and involved in the conformational change of MLKL, was identified as a putative UH15-binding residues

based on molecular modeling. In order to investigate the activation mechanism of necroptosis inducers and their interference on binding interaction, MEFs with mutation of M272W or S462A were generated by reexpressing mutated murine MLKL genes in MLKL^{-/-} MEFs. Since UH15-22 was among the most potent analog with low toxicity but high sensitivity (Fig. 3.4), it was selected to investigate the extent of necroptosis activation. When inducing MLKL expression by doxycycline, MEFs reconstituted with mutated MLKL of M272W or S462A presented comparable levels of MLKL as wild-type MLKL, confirmed by western blot analysis (Fig. 3.5A and C). It was revealed that both mutations had protective effects against necroptotic cell death in MEFs; however, both mutations failed to fully protect MEFs (Fig. 3.5B and D). The result suggests that both residues, Met²⁷² and Ser⁴⁶², may be involved in the interaction between RIPK3 and MLKL and functional in necroptosis activation.

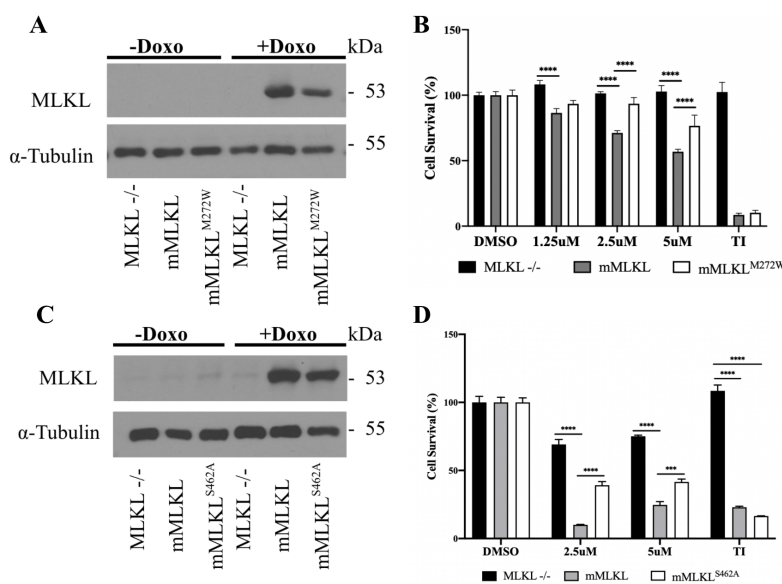


Fig. 3.5. Residues Met²⁷² and Ser⁴⁶² in murine MLKL affect necroptosis activation. MLKL^{-/-} MEFs were reconstituted with murine wild-type MLKL or (A) MLKL^{M272W} and (C) MLKL^{S462A}. MEFs were treated with or without 50 ng/mL doxycycline for 6hr. The expression level of MLKL was analyzed by western blot. MLKL^{-/-} MEFs, MEFs reconstituted with wild-type MLKL, and MEFs reconstituted with (B) MLKL^{M272W} and (D)

MLKL^{S462A} were treated with 50 ng/mL doxycycline for 6hr prior to indicated concentrations of UH15-22 or 10 ng/mL mTNF and 20 μM IDN6556. Survival rate was measured 24 hr after treatment by ATP assay. All the data are presented as mean ± SD of n=3 using Two-way ANOVA with Tukey's multiple comparison test.

3.2.3. Release of exosomes in response to UH15-22 mediated by RIPK3 and MLKL

Extracellular vesicles (EVs), released upon the inflammatory or immunogenic stimulation, are essential components in intracellular communication.²¹⁻²² Accompanied with the release of DAMPs and PAMPs, EVs provide signals to neighboring cells following tissue damage and trigger immune response.²² EVs can be classified as exosomes, microparticles, and apoptotic bodies depending on their size and biogenesis.²¹⁻²² Previous research has demonstrated that necroptotic cells release EVs by utilizing the ESCRT machinery.¹⁹ Therefore, it is important to examine whether key mediators of necroptosis, RIPK3 and MLKL, are associated with the release of EVs. RAW cells with the deficiencies of RIPK3, MLKL, or both were generated and the expression levels were confirmed by western blot analysis (Fig 3.6A). According to the result presented before, the mean size of EVs collected from 100,000 x g centrifugation were consistent with the typical size of exosomes,²² the EVs collected in our experiment were mostly exosomes. The exosomes released from UH15-22 induced RAW cells were only detected in the presence of RIPK3 after 190 min centrifugation, as shown by exosomal marker CD63, a tetraspanin found in most EVs (Fig 3.6B). To explore the regulation of RIPK3 and MLKL in a detailed manner, markers from different steps of EVs formation mechanism were tested. Early endosomal marker RAB5 and ESCRT-I complex component TSG101 were found in exosomes released from all RAW cells, but less in the absence of RIPK3 and MLKL after 190 min and overnight centrifugation (Fig 3.6B). Lysosomal marker VAMP7, on the other hand, was only found in exosomes released from cells with presence of RIPK3 after 190 min centrifugation (Fig 3.6B).

Based on these observations, RIPK3 was involved in the step downstream of multivesicular bodies formation, but the full extent release of exosomes requires the presence of both RIPK3 and MLKL.

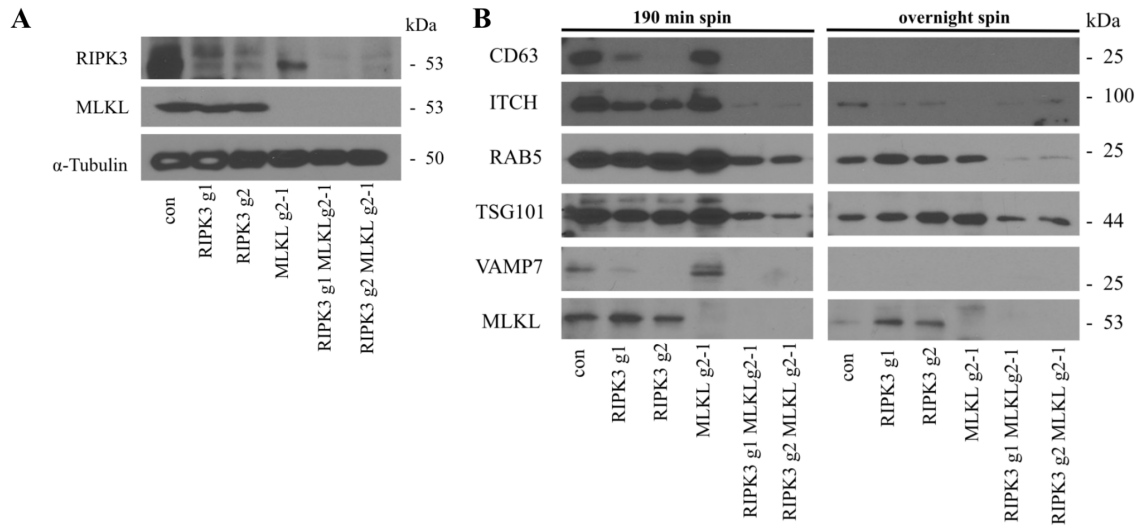


Fig 3.6. Release of exosomes induced by UH15-22 requires the presence of RIPK3 and MLKL. (A) RAW 264.7 cells were transduced by RIPK3 g1, RIPK3 g2, and MLKL g2-1 to introduce the knockout of RIPK3 and MLKL. The expression levels of RIPK3 and MLKL were presented by western blot analysis. (B) RAW 264.7 cells were treated with 2.5 μ M UH15-22 for 24 hr to collect extracellular vesicles twice. The expression levels of CD63, ITCH, RAB5, TSG101, VAMP7, and MLKL were shown by western blot analysis.

The XIAP g1 and cIAP2 g1 plasmid were gifts from Dr. Derek Abbott (Case Western Reserve University). All other plasmids were created and generated by Dr. Alexei Degterev. All experiments in this chapter were performed solely by myself.

Chapter 4: Discussion

4.1. Possible mechanisms of CS3/birinapant-mediated cell death

As the results indicated, CS3 and birinapant triggered cell death through a combination of cell death pathways. Both XIAP and RIPK1 were degraded and the deficiency of RIPK1 blocked the cell death pathways. It seems that the combination of CS3 and birinapant may promote a novel kind of cellular regulation which involves proteins in addition to RIPK1 and cIAP1. We hypothesized that CS3 and birinapant may form PROTAC, which consists of a protein of interest (POI) ligand connecting to an E3 ubiquitin ligase recruiting ligand through an optimal linker.²³ The ubiquitination machinery forms when E3 ubiquitin ligase binds to its ligand and brings POI into close proximity. The POI is ubiquitinated by E3 ubiquitin ligase and then recognized for degradation by proteasome.²³ In this circumstance, IAPs serve as E3 ubiquitin ligases which target the POI for degradation. The degradation of RIPK1, therefore, is an indicator of PROTAC mechanism activation. Birinapant and CS3 are ligands for cIAP1 and RIPK1, but currently it is difficult to figure out the specific mechanism and the optimal linker for this PROTAC system.

4.2. Putative effects of UH15 and ALD analogs on RIPK3 and MLKL

Both UH15 and ALD analogs induce necroptotic cell death with the presence of MLKL. Different RIPK3 inhibitor analogs have different efficiencies, which may result from the binding interaction between RIPK3 and chemical groups on RIPK3 inhibitor analogs. Due to the fact that the interaction occurs within the pseudokinase domain of MLKL, it is postulated that mutation on the pseudokinase domain will alter the interaction between RIPK3 and MLKL, thus promoting necroptotic cell death. Indeed,

our results showed that mutation on Met²⁷² of murine MLKL reduced the killing activity of UH15-22 to MEFs with the presence of MLKL, presumably by hindering the access into the MLKL pseudo-active center. In addition, the mutation on other domains of MLKL such as S462A, which caused the conformational change of MLKL, interferes with the interaction between RIPK3 and MLKL. Therefore, RIPK3 inhibitor analogs binding to RIPK3 triggers its binding affinity changes to MLKL, which is mediated by residues on the active site of MLKL. In other words, when studying the necroptotic cell death induced by the interaction between RIPK3 and MLKL, it is crucial to consider the residues on MLKL that may affect the binding interaction.

4.3. Future directions

For CS3/birinapant-mediated cell death, it is important to consider factors that strengthen the postulation about PROTACs. Knockout of the possible E3 ligases, such as XIAP or cIAP1/2, to exclude the factor causing RIPK1 degradation could be performed. Other possible reasons for XIAP degradation can be taken into account. For example, the binding of ARTS to XIAP induces allosteric conformational change and activates ubiquitination activity of XIAP, causing its degradation.²⁴

For the effects of UH15 and ALD analogs on interaction between RIPK3 and MLKL, the specific binding interaction will need to be elucidated. More RIPK3 inhibitor analogs will be tested to investigate how they affect the binding. Based on the results that MLKL mutations of M272W or S462A had partial protective effect, double mutation of these two residues can be generated to see whether it can fully protect the cells from necroptosis induced by RIPK3 inhibitor analogs. In addition, more residues on the active site can be analyzed.

Chapter 5: Bibliography

1. Bock FJ, Tait SW. Mitochondria as multifaceted regulators of cell death. *Nature Reviews Molecular Cell Biology*. 2019;21(2):85-100. doi:10.1038/s41580-019-0173-8
2. Bursch W, Ellinger A, Gerner CH, Fröhwein U, Schulte-Hermann R. Programmed cell Death (PCD): APOPTOSIS, AUTOPHAGIC PCD, or others? *Annals of the New York Academy of Sciences*. 2006;926(1):1-12. doi:10.1111/j.1749-6632.2000.tb05594.x
3. Chen J, Kos R, Garssen J, Redegeld F. Molecular Insights into the Mechanism of Necroptosis: The Necrosome as a Potential Therapeutic Target. *Cells*. 2019;8(12):1486. doi:10.3390/cells8121486
4. de Almagro MC, Vucic D. Necroptosis: Pathway diversity and characteristics. *Seminars in Cell & Developmental Biology*. 2015;39:56-62. doi:10.1016/j.semcd.2015.02.002
5. Meng M-B, Wang H-H, Cui Y-L, et al. Necroptosis in tumorigenesis, activation of anti-tumor immunity, and cancer therapy. *Oncotarget*. 2016;7(35):57391-57413. doi:10.18632/oncotarget.10548
6. Samson AL, Zhang Y, Geoghegan ND, et al. MLKL trafficking and accumulation at the plasma membrane control the kinetics and threshold for necroptosis. *Nature Communications*. 2020;11(1). doi:10.1038/s41467-020-16887-1
7. Berthelet J, Dubrez L. Regulation of apoptosis by inhibitors of apoptosis (iaps). *Cells*. 2013;2(1):163-187. doi:10.3390/cells2010163
8. Fulda S, Vucic D. Targeting IAP proteins for therapeutic intervention in cancer. *Nature Reviews Drug Discovery*. 2012;11(2):109-124. doi:10.1038/nrd3627
9. Abbas R, Larisch S. Targeting XIAP for Promoting Cancer Cell Death—The Story of ARTS and SMAC. *Cells*. 2020;9(3):663. doi:10.3390/cells9030663
10. Lalaoui N, Merino D, Giner G, et al. Targeting triple-negative breast cancers with THE Smac-mimetic birinapant. *Cell Death & Differentiation*. 2020;27(10):2768-2780. doi:10.1038/s41418-020-0541-0
11. Condon SM, Mitsuuchi Y, Deng Y, et al. Birinapant, a Smac-mimetic with IMPROVED tolerability for the treatment of solid tumors AND Hematological Malignancies. *Journal of Medicinal Chemistry*. 2014;57(9):3666-3677. doi:10.1021/jm500176w
12. Chang Y-C, Cheung CH. An updated review of Smac Mimetics, LCL161, Birinapant, And GDC-0152 in cancer treatment. *Applied Sciences*. 2020;11(1):335. doi:10.3390/app11010335
13. Fauster A, Rebsamen M, Huber KV, et al. A cellular screen identifies ponatinib and pazopanib as inhibitors of necroptosis. *Cell Death & Disease*. 2015;6(5). doi:10.1038/cddis.2015.130
14. Saussele S, Haverkamp W, Lang F, et al. Ponatinib in the treatment of Chronic myeloid leukemia and Philadelphia Chromosome-Positive Acute Leukemia: Recommendations of a German expert consensus panel with focus on Cardiovascular Management. *Acta Haematologica*. 2019;143(3):217-231. doi:10.1159/000501927

15. Najjar M, Suebsuwong C, Ray SS, et al. Structure guided design of potent and selective ponatinib-based hybrid inhibitors for ripk1. *Cell Reports*. 2015;10(11):1850-1860. doi:10.1016/j.celrep.2015.02.052
16. Weber K, Roelandt R, Bruggeman I, Estornes Y, Vandenameele P. Nuclear RIPK3 and Mkl1 contribute to cytosolic necrosome formation and necroptosis. *Communications Biology*. 2018;1(1). doi:10.1038/s42003-017-0007-1
17. Li J, McQuade T, Siemer AB, et al. The RIP1/RIP3 Necrosome forms a Functional Amyloid Signaling Complex required for Programmed necrosis. *Cell*. 2012;150(2):339-350. doi:10.1016/j.cell.2012.06.019
18. Davies KA, Fitzgibbon C, Young SN, et al. Distinct pseudokinase domain conformations underlie divergent activation mechanisms among vertebrate MLKL orthologues. *Nature Communications*. 2020;11(1). doi:10.1038/s41467-020-16823-3
19. Shlomovitz I, Yanovich-Arad G, Erlich Z, et al. Proteomic analysis OF necroptotic extracellular vesicles. 2020. doi:10.1101/2020.04.11.037192
20. Murphy JM, Lucet IS, Hildebrand JM, et al. Insights into the evolution of divergent nucleotide-binding mechanisms among Pseudokinases revealed by crystal structures of human and MOUSE MLKL. *Biochemical Journal*. 2014;457(3):369-377. doi:10.1042/bj20131270
21. Park SJ, Kim JM, Kim J, et al. Molecular mechanisms of biogenesis of apoptotic exosome-like vesicles and their roles as damage-associated molecular patterns. *Proceedings of the National Academy of Sciences*. 2018;115(50). doi:10.1073/pnas.1811432115
22. Baxter AA, Phan TK, Hanssen E, et al. Analysis of extracellular vesicles generated from monocytes under conditions of lytic cell death. *Scientific Reports*. 2019;9(1). doi:10.1038/s41598-019-44021-9
23. Sun X, Gao H, Yang Y, et al. Protacs: Great opportunities for academia and industry. *Signal Transduction and Targeted Therapy*. 2019;4(1). doi:10.1038/s41392-019-0101-6
24. Abbas R, Larisch S. Targeting XIAP for promoting cancer cell death—the story of arts And smac. *Cells*. 2020;9(3):663. doi:10.3390/cells9030663